Journal of Solid State Chemistry **156,** 321–324 (2001)
doi:10.1006/jssc.2000.9001, available online at http://www.idealibrary.com on IDEAL®

Crystal Structure of Li_3CuSbO_5

Sonia Trujillo T.,* Sylvain Bernès,†,[1] and María A. Castellanos R.*

*Facultad de Química, Laboratorio de rayos X, and †Facultad de Química, USAI, Dpto. de Química Analítica, Universidad Nacional Autónoma de México, Coyoacán 04510, D.F., México

Received June 26, 2000; in revised form September 8, 2000; accepted October 6, 2000; published online January 3, 2001

The structure of the complex oxide Li_3CuSbO_5 was determined by single-crystal X-ray diffraction at 0.71-Å resolution in space group $P\bar{1}$; $a = 5.1598(6)$, $b = 5.3798(7)$, $c = 7.7953(10)$ Å, $\alpha = 105.523(9)$, $\beta = 102.419(9)$, $\gamma = 103.411(10)^\circ$, $V = 193.74(4)$ Å^3, $Z = 2$, $R_1 = 2.41\%$ for 955 reflections having $I > 2\sigma(I)$ and w$R_2 = 5.22\%$ for 1107 independent reflections. The observed structure is based on close packing layers of oxide ions and is related with that of rock salt. © 2001 Academic Press

Key Words: **antimony; copper; lithium; oxide.**

INTRODUCTION

Studies in the ternary system Li_2O–CuO–Sb_2O5 show the formation of a pair of new complex oxides of formula Li_3CuSbO_5(O) and $Li_3Cu_2SbO_6$ (S) in the line Li_3SbO_4–CuO. Li_3SbO_4 presents a crystal structure determined in the space group $P2/c$ by Rietveld refinement. This structure is an ordered rock salt type, with distorted octahedra of oxide ions (1). The crystal structure of S was already characterized and determined by X-ray powder diffraction. It is monoclinic, space group $C2/c$ and has a partially ordered rock salt structure. This phase shows a low level of electronic conductivity (2).

Phase O, less rich in copper than phase S, seemed to be a good candidate to exhibit a rock salt derivative structure, too. The X-ray powder pattern data of phase O resisted all the attempts at Rietveld refinement, because it was very difficult to index. We succeed in the growth of fine, small single crystals of phase O. In this work we report the results of the single-crystal structure determination of phase O, Li_3CuSbO_5.

EXPERIMENTAL SECTION

Synthesis. Stoichiometric amounts of the reactants Li_2CO_3, Sb_2O_5, and CuO were ground in an agate mortar using acetone as vehicle and dried. The resultant mixture was fired in a platinum crucible. All reaction products were characterized by X-ray powder diffraction on a Siemens D5000 diffractometer using Cu$K\alpha$ radiation. Details of the synthesis of Li_3CuSbO_5 (O) by solid-state reaction were previously reported (3).

Crystallography. The structure of Li_3CuSbO_5 (O) was determined by single-crystal X-ray diffraction. Small green anhedral opaque crystals of Li_3CuSbO_5 were obtained by grain growth at the edges of a polycrystalline sample left in a platinum boat 3 weeks at 1125°C. From rotation photographs it was obvious that only the smaller grains were single crystals and diffraction data were measured on an irregular crystal of approximate dimensions $40 \times 20 \times 20$ μm, at room temperature, on a Siemens P4 diffractometer using graphite monochromated Mo$K\alpha$ radiation. Cell dimension refinement, Laue group determination, and data collection were achieved using common procedures (4). It should be mentioned that a pseudomonoclinic cell can be obtained by application of the transformation [− 1 − 1 0, − 1 − 1 − 2, 1 0 0] to the original cell. However, no crystal actually presented the $2/m$ Laue symmetry. Because of the strong diffracting power of the crystal, data were collected up to $2\theta = 60^\circ$ and a complete sphere (eight octants) was measured and merged, in order to determine accurately the parameters of the light Li atoms. Raw data were corrected for absorption on the basis of 50 ψ-scans measured with χ close to 90°. Density measurements of polycrystalline material were made in a pycnometer bottle by displacement of CCl_4 at room temperature and confirmed that $Z = 2$ for the $P\bar{1}$ space group.

The structure was solved from a Patterson map interpretation (5) (Sb atom) and Fourier difference maps (remaining atoms). A structural disorder was observed for the Cu2 atom which is disordered with Li2. Site occupation factors were refined for these atoms and fixed to $\frac{1}{2}$ in the last refinement cycles. Complete model was refined without constraints nor restraints with anisotropic thermal parameters for Sb, Cu, and O atoms. Li atoms were refined isotropically due to a tendency to converge to nonpositive definite

[1] Present address: Centro de Química, Instituto de Ciencias, Universidad Autónoma de Puebla, Blvd. 14 sur 6303, Col. San Manuel, 72570 Puebla, Pue., México.

0022-4596/01 $35.00

thermal ellipsoids. A convenient weighting scheme and a correction for extinction were applied to the data. Pertinent crystallographic data are reported in Table 1, while final atomic parameters and principal geometric results are presented in Tables 2 and 3. Anisotropic displacement coefficients are displayed in Table 4. The graphic material was prepared using CaRIne software (6) and SHELXTL (7). The unit cell is described in Fig. 1. Complete data and structure factors in a CIF format are available on request. The calculated powder pattern of phase O was obtained with CaRIne (6) and was observed to be basically identical to the experimental one registered on a Siemens D5000 diffractometer.

RESULTS AND DISCUSSION

The crystalline structure of O is based on close packing layers of oxide ions and related with that of rock salt. The distortion from the cubic cell of the rock salt to the observed triclinic is due to the fact that the three cations included in phase O, Li^+, Cu^{2+}, and Sb^{5+} are very different and consequently distort the cubic close packing in very different ways in their immediate environment.

The overall structure is formed by the association of cation octahedra sharing edges arranged in two distinct layers approximately normal to the *b* axis of the triclinic cell. One layer contains isolated [CuO_6] octahedra surrounded by six [LiO_6] octahedra forming a hexagonal ring (see Fig. 2, layer A on Fig. 4). A Cu ion is located on an inversion

TABLE 1
Summary of Crystallographic Data for Li_3CuSbO_5

Empirical Formula	$CuLi_3O_5Sb$
Space group	$P\bar{1}$
a(Å)	5.1598(6)
b(Å)	5.3798(7)
c(Å)	7.7953(10)
α(°)	105.523(9)
β(°)	102.419(9)
γ(°)	103.411(10)
Volume(Å^3)	193.74(4)
Z	2
Density (calc.) (g cm^{-3})	4.904
Measured density (g cm^{-3})	4.641
Absorption coefficient (mm^{-1})	12.356
F(000)	258
2θ Range (°)	5.68 − 59.92
Index ranges	$-7 \le h \le 7, -7 \le k \le 7, -10 \le l \le 10$
Reflections collected	2214
Independent reflections[a]	1107 ($R_{int} = 4.18\%$)
Reflections with $F_o > 4\sigma(F_o)$	955
Transmission factors	min = 0.262, max = 0.340
Final R indices [$I > 2\sigma(I)$][a]	$R_1 = 2.41\%$, wR_2 = 4.88%
Final R indices (all data)[a]	$R_1 = 3.40\%$, w$R_2 = 5.22\%$
Goodness-of-fit on F^2, S[a]	1.030
Largest and mean Δ/σ	0.001, 0.000
Largest difference peak and hole (e Å^{-3})	0.895, − 0.914

[a] $R_{int} = \frac{\sum|F_o^2 - \langle F_o^2\rangle|}{\sum F_o^2}$, $R_1 = \frac{\sum||F_o| - |F_c||}{\sum|F_o|}$, $wR_2 = \sqrt{\frac{\sum w(F_o^2 - F_c^2)^2}{\sum w(F_o^2)^2}}$, $S = \sqrt{\frac{\sum w(F_o^2 - F_c^2)^2|}{m - n}}$.

TABLE 2
Final Atomic Parameters for Li_3CuSbO_5

Atom	Site	X/a	Y/b	Z/c	U(eq)
Sb1	2*i*	0.1085(1)	0.7018(1)	0.7030(1)	0.005(1)
Cu1	1*c*	0	$\frac{1}{2}$	1	0.008(1)
Cu2[a]	2*i*	− 0.2968(6)	0.8902(7)	0.9011(4)	0.007(1)
Li2[a]	2*i*	− 0.3410(80)	0.8980(110)	0.8940(70)	0.004(9)
O1	2*i*	0.1333(7)	0.3335(7)	0.5475(4)	0.007(1)
O2	2*i*	0.3348(7)	0.6728(8)	0.9323(4)	0.011(1)
O3	2*i*	− 0.2151(8)	0.4946(8)	0.7601(5)	0.008(1)
O4	2*i*	0.4466(8)	0.8913(8)	0.6610(5)	0.009(1)
O5	2*i*	0.0547(7)	1.0430(7)	0.8340(5)	0.010(1)
Li1	1*h*	$\frac{1}{2}$	$\frac{1}{2}$	$\frac{1}{2}$	0.019(3)
Li3	2*i*	− 0.5840(20)	0.2940(20)	0.8036(13)	0.010(2)
Li4	2*i*	0.7720(20)	1.0990(20)	0.6113(13)	0.017(2)

[a] Site occupation factors for Cu2 and Li2: $\frac{1}{2}$. U(eq) is defined as one-third of the trace of the orthogonalized U_{ij} tensor.

TABLE 3
Selected Bond Lengths for Li_3CuSbO_5

Sb1–O1	2.076(4)	Sb1–O1 #1	2.013(3)
Sb1–O2	1.980(3)	Sb1–O3	1.988(4)
Sb1–O4	1.947(4)	Sb1–O5	1.960(4)
Cu1–O2	2.009(3)	Cu1–O2 #3	2.009(3)
Cu1–O3	1.947(4)	Cu1–O3 #3	1.947(4)
Cu1–O5 #4	2.564(4)	Cu1–O5 #5	2.564(4)
Cu2–O2 #5	2.437(5)	Cu2–O2 #6	2.088(4)
Cu2–O3	2.297(5)	Cu2–O4 #6	2.050(5)
Cu2–O5	2.046(5)	Cu2–O5 #5	2.059(5)
Li2–O2 #5	2.33(5)	Li2–O2 #6	1.96(5)
Li2–O3	2.44(5)	Li2–O4 #6	1.89(5)
Li2–O5	2.20(4)	Li2–O5 #5	2.20(5)
Li1–O1	2.053(3)	Li1–O3 #1	2.246(4)
Li1–O4	2.255(4)		
Li3–O1 #2	2.298(11)	Li3–O2 #2	2.197(10)
Li3–O2 #3	2.116(10)	Li3–O3	2.102(10)
Li3–O4 #7	2.211(10)	Li3–O5 #7	2.134(10)
Li4–O1 #7	2.229(11)	Li4–O1 #8	2.536(11)
Li4–O5 #2	2.152(11)	Li4–O3 #10	2.112(11)
Li4–O4	1.962(11)	Li4–O4 #9	2.199(10)

Note. Symmetry transformations used to generate equivalent atoms: #1, $-x, -y+1, -z+1$; #2, $x+1, y, z$; #3, $-x, -y+1, -z+2$; #4, $x, y-1, z$; #5, $-x, -y+2, -z+2$; #6, $x-1, y, z$; #7, $x-1, y-1, z$; #8, $-x+1, -y+1, -z+1$; #9, $-x+1, -y+2, -z+1$; #10, $x+1, y+1, z$.

TABLE 4
Anisotropic Displacement Coefficients ($Å^2 \times 10^3$)

Atom	U_{11}	U_{22}	U_{33}	U_{23}	U_{13}	U_{12}
Sb(1)	6(1)	5(1)	4(1)	2(1)	2(1)	1(1)
Cu(1)	8(1)	11(1)	6(1)	5(1)	2(1)	1(1)
Cu(2)	4(1)	10(1)	5(1)	3(1)	0(1)	2(1)
O(1)	10(2)	5(2)	5(1)	1(1)	1(1)	3(1)
O(2)	9(2)	15(2)	10(2)	6(2)	3(2)	3(2)
O(3)	7(2)	12(2)	9(1)	6(1)	4(1)	3(1)
O(4)	5(2)	9(2)	9(2)	5(1)	2(1)	− 2(1)
O(5)	12(2)	10(2)	9(2)	3(1)	6(1)	5(2)

Note. The anisotropic displacement exponent takes the form: $-2\pi^2(h^2a^{*2}U_{11} + \cdots + 2hka^*b^*U_{12})$.

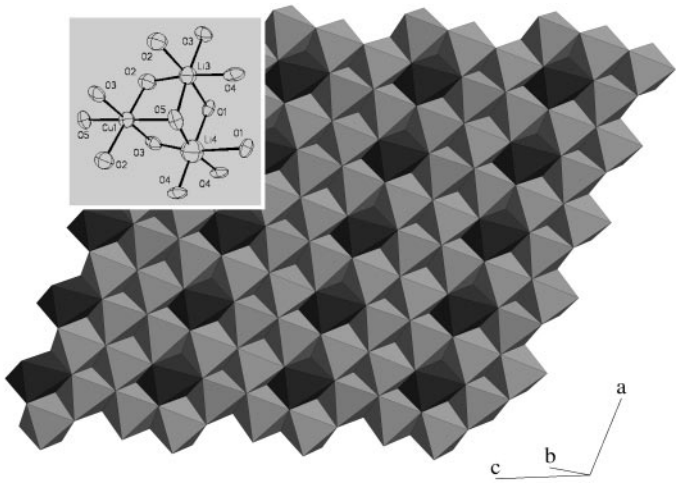

FIG. 2. Layer A in Li_3CuSbO_5 oxide projected almost down to the *b* axis of the cell. Dark octahedron correspond to the $[CuO_6]$ octahedra and the remaining to the $[LiO_6]$ octahedra. The inset shows an ORTEP view (7) for Cu1, Li3, and Li4 coordination environments, including thermal ellipsoids at 99.5% probability level. For clarity, inset and figure are at different scales but in the same orientation.

center and a Jahn–Teller effect is observed for the $[Cu1O_6]$ octahedra, with two apical Cu–O bond lengths of 2.564(4) while the other four bond lengths are in the range of 1.947(4) to 2.009(3) Å. Two distinct environments for Li^+ ions are observed in this layer as distorted octahedra: $[Li3O_6]$ with distances in the range 2.102(10) to 2.298(11) Å and $[Li4O_6]$ with distances in the range 1.962(11) to 2.536(11) Å. This last one is more distorted because the $[Li4O_6]$ octahedra share two edges with the $[Cu1O_6]$ octahedra. As a consequence of the compensation between the Jahn–Teller effect for Cu1 and the distortion for Li4 environment, the building of layers with these ions is observed.

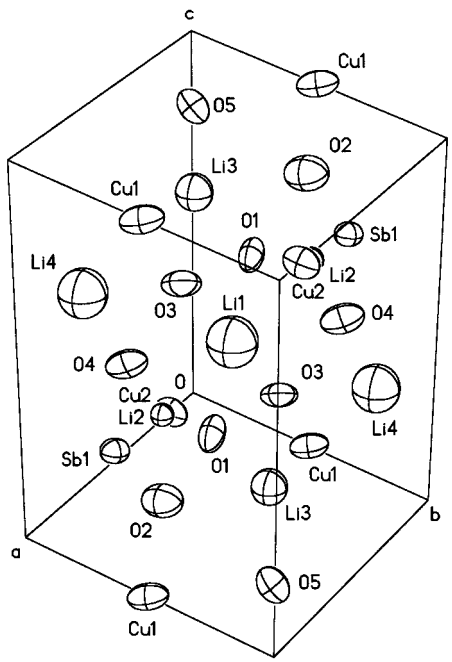

FIG. 1. Distribution of atomic positions in the unit cell of Li_3CuSbO_5 (O) with numbering scheme. Thermal ellipsoids (7) are at 99.5% probability level. Note that Li atoms are isotropically refined. Cu2 and Li2 are disordered with occupation factors of $\frac{1}{2}$ but refined as independent positions.

The second layer (Fig. 3, layer B on Figure 4), parallel to that previously described, is characterized by zig-zag chains of $[MO_6]$ octahedra where *M* is a 1 : 1 mixture of Cu^{2+} and Li^+ ions, running along the *a* axis. This structural disorder is attributable to the close values of the ionic radii for Li^+ and Cu^{2+} in octahedral coordination, 0.76 and 0.73 Å, respectively (8). These chains are linked by pairs of $[SbO_6]$ octahedra and the isolated $[Li1O_6]$ octahedra (Fig. 3). Each

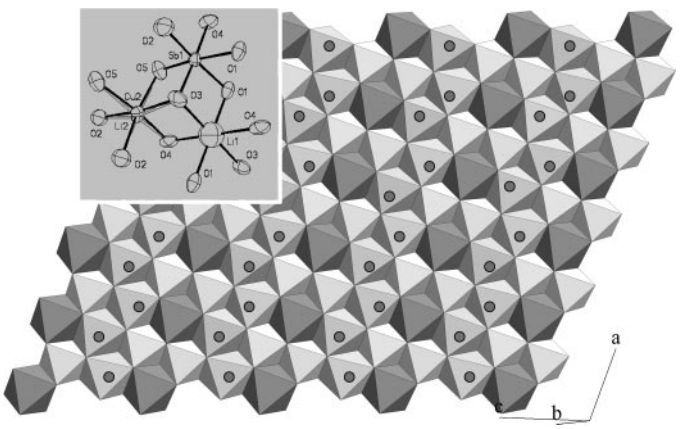

FIG. 3. Layer B in Li_3CuSbO_5 oxide projected almost down to the *b* axis of the cell. White octahedra contain Sb cation, dotted octahedra belong to the $[MO_6]$ octahedron, where *M* is 1:1 Cu/Li cation and the gray octahedra are $[LiO_6]$. The inset shows an ORTEP view (7) for Sb1, Cu2/Li2, and Li1 coordination environments, including thermal ellipsoids at 99.5% probability level. For clarity, inset and figure are at different scales but in the same orientation.

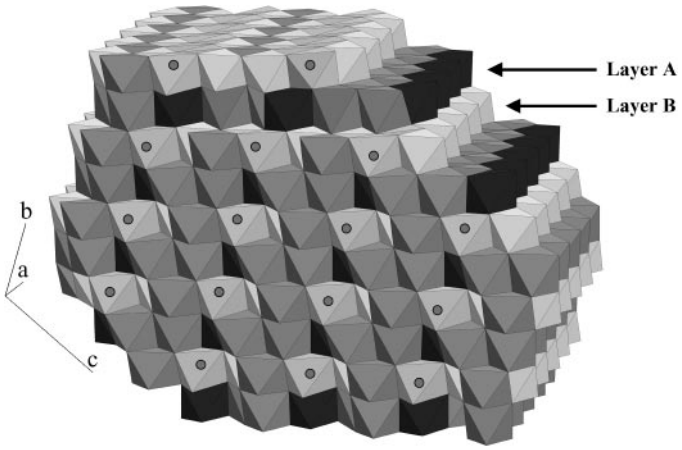

FIG. 4. Complete structure Li_3CuSbO_5 oxide, described as an array of octahedra. The representation of octahedra is the same as for previous figures.

$[Li1O_6]$ octahedron is surrounded by a hexagon of two pairs of $[SbO_6]$ and two $[MO_6]$ of neighboring zig-zag chains. The Cu2/Li2 site presents a minor Jahn–Teller effect in comparison to that observed for Cu1, with Cu–O bond lengths ranging from 2.046(5) to 2.437(5) Å. It should be mentioned that the Li2 ion disordered with Cu2 presents very large standard deviations for its position (see Table 2) in spite of normal thermal parameters (see Table 4). This effect is not observed for the remaining Li atoms in the structure. This difference may be a measure of the delocalization of this cation in the solid. This can be appreciated by the fact that atomic positions for Cu2 and Li2 were determined from structure refinement as distinct sites, in spite of the short final interatomic distance in the structure, Cu2–Li2 = 0.24(4) Å. The Sb environment is close to a regular octahedron with Sb–O bond lengths ranging from 1.947(4) to 2.076(4) Å, similar to those reported for related compounds (9, 10), although less regular than the equivalent octahedron for the S compound (2). The $[Li1O_6]$ octahedra present a distortion similar to that of Li3, with Li–O distances between 2.053(3) and 2.255(4) Å. Nevertheless, this polyhedron can be considered as the more regular of this structure, due to the special position of Li1 which restrains the *trans* angles to have the ideal value of 180° (see Table 2).

The stacking of the previously described layers approximately along the *b* axis in an alternate manner forms the complete structure described in Fig. 4. Five crystallographic independent oxide ions are forming the close packed layers in this structure. The sequence of cations between the oxide close packed layers is also apparent in the unit cell: (Cu–Li–Li–Li–Li …) and (Sb–Cu/Li–Li–Cu/Li–Sb …) (see Figs. 1, 2, and 3). Each oxygen atom has different octahedral coordination with the cations Li^+, Cu^{2+}, Li^+/Cu^{2+}, and Sb^{5+}, as commonly observed in the rock-salt-type structures. The local electroneutrality is satisfied in distinct manners for each oxygen atom: the variation in charge ranges from 1.75 + for O4 to 2.33 + for O1, while O2 and O5 remain with the expected charge 2 + .

The calculated bond valences and bond valence sums (BVS) (11) for each atom are 0.96 + , 1.33 + , 1.91 + , and 4.69 + for Li^+, Cu^{2+}/Li^+, Cu^{2+}, and Sb^{5+}, respectively. These values are close to the expected atomic valence, which is evidence of the correctness of the structure. The major deviation for the atomic charge is observed for antimony and can be related with the distortion of the octahedron of this cation.

The close packed layers of oxide ions and cations in the triclinic cell of phase O (see Fig. 1) yields a packing index close to that of the rock salt, 68%. Both structures are related with all the octahedral interstices occupied and the sharing of the 12 edges of each octahedron.

By comparison with Li_3SbO_4 (1) and $Li_3Cu_2SbO_6$ (S) (2), the reported structure for Li_3CuSbO_5 (O), can be considered as a structural intermediate: while in the first one $[SbO_6]$ octahedra form infinite zig-zag chains, in the second, S, the octahedra are isolated. In phase O, an intermediate situation is observed, with isolated pairs of $[SbO_6]$. Besides, in going from O to S the zig-zag Cu/Li chains are broken and the same happens to the pair of $[SbO_6]$ octahedra with an increasing amount of copper. An important difference between S and O is the sharing of $[LiO_6]$ and $[MO_6]$ octahedra faces for S which is not observed for O. In spite of these differences, the packing indexes remain the same.

ACKNOWLEDGMENTS

S.B. is grateful to USAI (UNAM) for diffractometer time. PAPIIT program is acknowledged for funding this work (Grant IN-107398).

REFERENCES

1. J. M. S. Skakle, M. A. Castellanos R., S. Trujillo Tovar, S. M. Fray, and A. R. West, *J. Mater. Chem.* **6,** 1939–1942 (1996).
2. J. M. S. Skakle, M. A. Castellanos R., S. Trujillo Tovar, and A. R. West, *J. Solid State Chem.* **131,** 115–120 (1997).
3. M. A. Castellanos R., S. Trujillo T., J. M. S. Skakle, and A. R. West, *MRS Symp. Proc.* **453,** 159–164 (1997).
4. J. Fait, "XSCANS Users Manual." Siemens Analytical X-ray Instruments Inc., Madison, WI, 1991.
5. G. M. Sheldrick, "SHELX97 Users Manual." Univ. of Göttingen, Germany, 1997.
6. C. Boudias and D. Monceau, "CaRIne Crystallography," Release 3.1, 1998.
7. G. M. Sheldrick, "SHELXTL-plus," Release 5.10. Siemens Analytical X-ray Instruments Inc., Madison, WI, 1998.
8. R. D. Shannon, *Acta Crystallogr. A* **32,** 751 (1976).
9. J. L. Fourquet, P. A. Giles, and A. Le Bail, *Mater. Res. Bull.* **24,** 1207–1214 (1989).
10. C. Greaves and S. M. A. Katib, *Mater. Res. Bull.* **25,** 1175–1182 (1990).
11. I. D. Brown, *in* "Structure and Bonding in Crystals" (M. O'Keeffe and A. Navrotsky, Eds.), Vol. II. Academic Press, San Diego, 1981.